Atomistic theory of the shear band direction in amorphous solids

Ashwin J.[1], Oleg Gendelman[2], Itamar Procaccia[1] and Carmel Shor[1]
[1] *Department of Chemical Physics, The Weizmann Institute of Science, Rehovot 76100, Israel*
[2] *Faculty of Mechanical Engineering, Technion, Haifa 32000, Israel.*
(Dated: April 16, 2013)

One of the major theoretical riddles in shear banding instabilities is the angle that the shear band chooses spontaneously with respect to the principal stress axis. Here we employ our recent atomistic theory to compute analytically the angle in terms of the characteristics of the Eshelby inclusion that models faithfully the eigenfunction of the Hessian matrix that goes soft at the plastic instability. We show that loading protocols that do not conserve volume result in shear bands at angles different from 45^o to the strain axis; only when the external strains preserve volume like in pure shear, the shear bands align precisely at 45^o to the strain axis. We compute an analytic formula for the angle of the shear band in terms of the characteristics of the loading protocol; quantitative agreement with computer simulations is demonstrated.

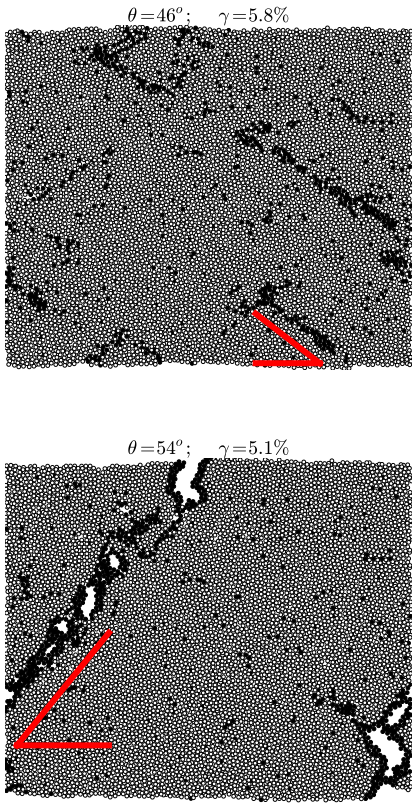

FIG. 1. Color Online: The shear band that occurs in a 2-dimensional amorphous solid upon uniaxial compression (upper panel) and extension (lower panel). The angle with respect to the principal stress component measured in the upper panel is $46^o \pm 1^0$, whereas in the lower panel it is $54^o \pm 1^0$. This Letter provides a microscopic theory of this asymmetry.

The riddle that this Letter aims to solve is demonstrated in Fig. 1. Amorphous solids put under different loading conditions display shear bands that appear at different angles with respect to the principal stress axis [1]. In past work phenomenological models were applied to this riddle [2–4], but a microscopic approach was lacking. In this Letter we provide a microscopic theory of this phenomenon in athermal systems that are strained under quasi-static conditions [5, 6]. The Letter culminates with an analytic formula for the angle in terms of one parameter which is determined by the loading conditions. For simplicity and concreteness we will explain the theory in 2-dimensions, the generalization to 3-dimension is available [7].

Recently there had been rapid progress in understanding the nature of plastic instabilities in Athermal Quasistatic (AQS) conditions [8–12]. Consider a glass-forming system made of N particles interacting via generic potentials (i.e. at least twice differentiable everywhere). The total energy can be written at $T = 0$ in terms of the positions $\boldsymbol{r}_1, \boldsymbol{r}_2, \cdots \boldsymbol{r}_N$ of these particles, $U = U(\boldsymbol{r}_1, \boldsymbol{r}_2 \cdots, \boldsymbol{r}_N)$. The Hessian matrix is defined as the second derivative [13]

$$H_{ij} \equiv \frac{\partial^2 U(\boldsymbol{r}_1, \boldsymbol{r}_2 \cdots, \boldsymbol{r}_N)}{\partial \boldsymbol{r}_i \partial \boldsymbol{r}_j} \ . \tag{1}$$

The Hessian is real and symmetric, and therefore can be diagonalized. Excluding Goldstone modes whose eigenvalues are zero due to continuous symmetries, all the other eigenvalues are real and positive as long as the system is mechanically stable. In equilibrium, without any mechanical loading, eigenfunctions associated with large eigenvalues are localized due to Anderson localization. But all the eigenfunctions associated with low eigenvalues (including all the excess modes that are typical to amorphous solids) are extended. At *low values of external loading* one observes "fundamental plastic instabilities" when eigenvalues of some modes approach zero via a saddle node bifurcation [14]. Simultaneously the associated eigenfunction localizes on a typical quadrupolar structure (in both 2 and 3 dimensions) that is identical to the non-affine displacement field associated with the plastic event. An example of such a localized eigenfunction that is seen upon uniaxial compression is shown in Fig. 2. At higher values of the external strain the nature of the plastic instability can change drastically.

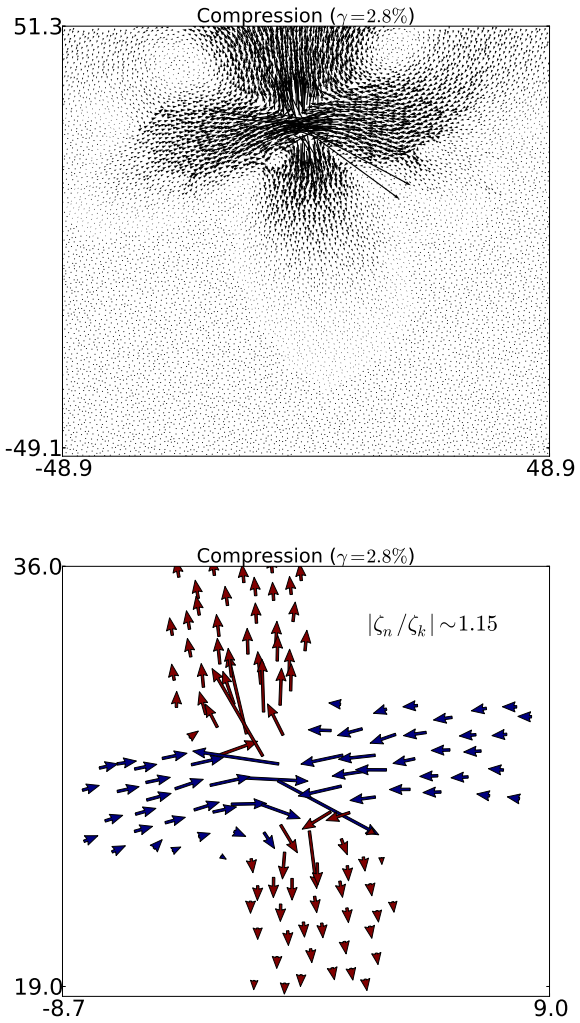

FIG. 2. Upper panel: A fundamental plastic event during an AQS uniaxial compression simulation of a 2-dimensional amorphous solid. Shown is the non-affine displacement field in the whole system. Lower panel: a small window around the core of the event shown in the upper panel. For clarity we show only the incoming and outgoing arrows.

For well quenched amorphous solids one finds that instead of single fundamental events there exists a bifurcation to the simultaneous appearance of a finite *density* of such events, (i.e. infinity of them in the thermodynamic limit), and that in two dimensions they organize along a line [11, 12]. In previous work the angle of this line with respect to the principal stress axis was calculated analytically for external shear, with the result of 45^o. We will explain now why external shear is special, and why the angle will change for other loading conditions.

A very important realization is that the fundamental plastic event can be excellently modeled analytically as an Eshelby inclusion [15]. As is well known, the Eshelby construction in 2-dimensions starts with a circle taken out from an elastic medium, made into an ellipse that is then pushed back to the medium. This is the Eshelby inclusion. In terms of the two orthogonal directions $\hat{\boldsymbol{n}}$ and $\hat{\boldsymbol{k}}$ one writes the eigenstrain of the inclusion as

$$\epsilon^*_{\alpha\beta} = \zeta_n \hat{n}_\alpha \hat{n}_\beta + \zeta_k \hat{k}_\alpha \hat{k}_\beta \ . \tag{2}$$

The "eigenvalues" ζ_n and ζ_k characterize the relative magnitude of the non-affine displacement associated with the fundamental plastic instability. The direction $\hat{n}$ is that of the principal stress axis, and $\hat{k}$ the orthogonal one. The ratio $|\zeta_n/\zeta_k|$ depends, as shown below, on the loading conditions. When area preserving prevails, $\zeta_n = -\zeta_k$ [11, 12], but in general these numbers are independent, and their ratio characterizes the loading condition. We argue below that this ratio determines uniquely the angle of the shear band once there appears a density of such events with a prescribed ratio $|\zeta_n/\zeta_k|$.

Having the eigenstrain (2) one asks what is the displacement field associated with such an inclusion. The calculation is shown in detail in the accompanying material [16], with the final result

$$\begin{aligned}\boldsymbol{u}^c(\boldsymbol{X}) = \frac{(\zeta_n-\zeta_k)(\lambda+\mu)}{4(\lambda+2\mu)}\left(\frac{a^2}{r^2}\right)\Bigg[2\frac{(\zeta_n+\zeta_k)}{(\zeta_n-\zeta_k)}\boldsymbol{X} + \left(\frac{2\mu}{\lambda+\mu}+\frac{a^2}{r^2}\right)\Big(2(\hat{\boldsymbol{n}}\cdot\boldsymbol{X})\hat{\boldsymbol{n}} - \boldsymbol{X}\Big) \\ + 2\left(1-\frac{a^2}{r^2}\right)\Big(2(\hat{\boldsymbol{n}}\cdot\hat{\boldsymbol{r}})^2-1\Big)\boldsymbol{X}\Bigg]\end{aligned} \tag{3}$$

with $\boldsymbol{X}$ denoting an arbitrary Cartesian point in the material, $r = |\boldsymbol{X}|$, $\hat{\boldsymbol{r}} \equiv \boldsymbol{X}/r$ and a is a parameter known as the "core size". The stress field induced by this displacement field is denoted below as $\sigma^c_{\alpha\beta}$.

As said above under simple shear one conserves area, and $\zeta_n = -\zeta_k$. Thus the first term inside the square parenthesis in Eq. 3 vanishes, and in the two other terms $\zeta_n - \zeta_k = 2\zeta_n \equiv \epsilon$, cf. [12]. We have seen in Ref. [12], and we will see below, that when such a condition applies, the angle of the shear band is precisely 45^o with respect to

the principal stress axis. But for the more general loading conditions in which $\zeta_n \neq -\zeta_k$ the angle is different, see Eq. (15) below.

When the amorphous solid is well quenched, the nature of the plastic instability changes when the external strain becomes sufficiently high; a density of inclusions of the form (3) appear simultaneously. To find their geometrical organization we need to compute the energy of such $\mathcal{N}$ inclusion in a system of total volume V and minimize it with respect to their orientation and geometry. The total energy of such $\mathcal{N}$ inclusion has four contributions:

$$E = E_{mat} + E_{\infty} + E_{esh} + E_{inc} \tag{4}$$

with each component of energy defined as

$$E_{mat} = \frac{1}{2}\sigma^{\infty}_{\alpha\beta}\epsilon^{\infty}_{\beta\alpha}V \tag{5}$$

$$E_{\infty} = -\frac{1}{2}\sigma^{\infty}_{\alpha\beta}\sum_{i=1}^{N}\epsilon^{*,i}_{\beta\alpha}V_0^i \tag{6}$$

$$E_{esh} = \frac{1}{2}\sum_{i=1}^{N}(\sigma^{*,i}_{\alpha\beta} - \sigma^{c,i}_{\alpha\beta})\epsilon^{*,i}_{\beta\alpha}V_0^i \tag{7}$$

$$E_{inc} = -\frac{1}{2}\sum_{i=1}^{N}\epsilon^{*,i}_{\beta\alpha}V_0^i\sum_{j\neq i}\sigma^{c,j}_{\alpha\beta}(r^{ij}) \ . \tag{8}$$

Here the eigen-strain $\epsilon^{*,i}_{\alpha\beta}$ and volume V_0^i associated with any i^{th} Eshelby inclusion are given as

$$\begin{aligned} V_0^i &= \pi a^2 \\ \epsilon^{*,i}_{\alpha\beta} &= \frac{(\zeta_n - \zeta_k)}{2}(2\hat{n}^i_\alpha\hat{n}^i_\beta - \delta_{\alpha\beta}) + \frac{(\zeta_n + \zeta_k)}{2}\delta_{\alpha\beta} \end{aligned} \tag{9}$$

The reader should recognize that the first contribution, (5), is the energy of the elastic matrix and the second ((6)) is the energy due to the interaction of the elastic matrix with the inclusions. The third, (7), is the self-energy of all the inclusions, and the last, (8), is the interaction energy of different inclusions.

Also for a 2D material being loaded under uni-axial strain with free boundaries along $\hat{y}$, we can write the form of the global stress tensor as

$$\sigma^{\infty} = \begin{pmatrix} \sigma^{\infty}_{xx} & 0 \\ 0 & 0 \end{pmatrix} \ . \tag{10}$$

By Hooke's law, we get the expression for applied global stress tensor using the Lamé coefficients λ and μ:

$$\sigma^{\infty}_{\alpha\beta} = \lambda\epsilon^{\infty}_{\eta\eta}\delta_{\alpha\beta} + 2\mu\epsilon^{\infty}_{\alpha\beta} \ . \tag{11}$$

Taking trace of Eq. (11), we find

$$\epsilon^{\infty}_{\eta\eta} = \frac{1}{2(\lambda+\mu)}\sigma^{\infty}_{\eta\eta} = \frac{1}{2(\lambda+\mu)}\sigma^{\infty}_{xx} \tag{12}$$

Plugging Eq. (12) in Eq. (11), we find

$$\sigma^{\infty}_{xx} = \frac{4\mu(\lambda+\mu)\gamma}{\lambda+2\mu} \tag{13}$$

where γ is the external strain.

Clearly, the first contribution Eq. (5) is independent of the distribution of inclusions and will not affect the state of minimal energy. The second term Eq. (6) is the only one proportional to the external strain γ, and therefore for sufficiently large γ it needs to be minimized first. Besides γ, this term depends only on the orientation of each inclusion, i.e. on the angle $\phi = \cos^{-1}(n^i_x) = \sin^{-1}(n^i_y)$. Minimizing the term with respect to this angle we find that the minimum is obtained when $\phi = 0$ or $\pi/2$. In other words, each inclusion is oriented with one axis parallel and the other orthogonal to the uniaxial direction. Plugging this information into Eqs. (7) and (8) simplifies them considerably, and see the supplementary material for full details [16]. The organization and orientation of the density of inclusions is determined by minimizing $E_{\rm inc}$ of Eq. (8). The minimum energy is obtained when all the inclusions align on a line that is at an angle θ with respect to the uniaxial direction [16]. The final prediction for this angle is

$$\cos^2\theta = \frac{1}{2} - \frac{\zeta_n + \zeta_k}{4(\zeta_n - \zeta_k)} \ , \tag{14}$$

or

$$\theta = \cos^{-1}\sqrt{\frac{1}{2} - \frac{\zeta_n + \zeta_k}{4(\zeta_n - \zeta_k)}} \ . \tag{15}$$

One learns immediately from Eq. (15) that the area preserving case, $\zeta_n = -\zeta_k$, leads to an angle of precisely 45^o. Any other loading condition would result in a different angle. The two extreme cases occur for $|\zeta_n/\zeta_k| \to 0$ and $|\zeta_n/\zeta_k| \to \infty$. The first case would realize an angle of 30^o and the second an angle of 60^o. All experimental realizations should fall between these two extreme universal limits without exception. Indeed, examining the wide range of angles reported in Ref. [1] we see that all the data falls within our theoretical limits. We return now to our simulations shown in Fig. 1 to rationalize the angles observed.

In order to understand the angle seen in a particular experiment one needs to figure how the values of ζ_n and ζ_k are determined by the loading conditions. For example in uniaxial extension the outgoing direction may become highly dominant compared to the incoming one, leading to a high ratio of $|\zeta_n/\zeta_k|$. This is not the case for compression, as one can see from Fig. 2. We expect such asymmetry to appear in any generic potential due to the steep rise of the repulsive part vs the moderate attractive tail. The ratio of eigenvalues is obtained from the lower panel by averaging the length of the incoming and outgoing vectors around the core. We find that the ratio of the average length provides a fair estimate of $|\zeta_n/\zeta_k|$, in this case $|\zeta_n/\zeta_k| \approx 1.15$. Using this value in Eq. (15) we find an angle $\theta \approx 46^o$ in perfect agreement with the observed angle in Fig. 1 upper panel. The exercise is

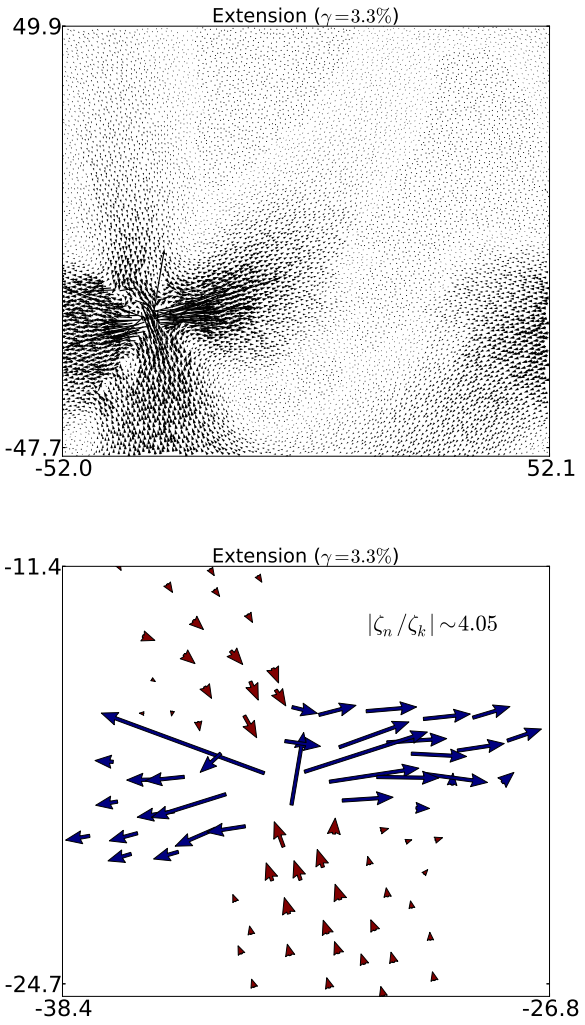

FIG. 3. Upper panel: A fundamental plastic event during an AQS uniaxial extension simulation of a 2-dimensional amorphous solid. Shown is the non-affine displacement field in the whole system. Lower panel: a small window around the core of the event shown in the upper panel. For clarity we show only the incoming and outgoing arrows.

repeated for uniaxial extension, see Fig. 3. Obviously, in the extension case the outgoing arrows are much longer than the incoming ones. Averaging the length of the outgoing and incoming vectors and taking the ratio we find for the present case $|\zeta_n/\zeta_k| \approx 4.05$. Plugging this value into Eq. (15) we get in this case $\theta \approx 54^o$, again in perfect accord with the observed angle in Fig. 1 lower panel.

To summarize, we note that the atomistic theory is based in the understanding that shear localization occurs due to a plastic instability in which a density of Eshelby-like quadrupolar structures organize on a line. Each individual quadrupolar structure is sensitive to the loading conditions, parameterized in the 2D case by the ratio of "eigenvalues" ζ_n/ζ_k. At zero temperature and under quasi-static conditions one is well justified to find the preferred geometry by energy minimization. This leads to the prediction that all the quadrupoles have the same orientation (for sufficiently high external strain) and that they organize on a line at an angle θ with respect to the principal stress axis. The angle θ is limited in this theory to fall between 30^o and 60^o, with 45^o being special to the area preserving situation $\zeta_n/\zeta_k = -1$. This range of allowed angles appears to be well in accord with published experimental results.

We have considered in detail the orientation of the shear bands under uniaxial compression and extension and demonstrated the sensitivity of the ratio of 'eigenvalues' to these different loading conditions. Finally, we showed that the theoretical prediction Eq. (15) is in excellent agreement with the observed angles in these loading conditions.

The extension of the theory to finite temperatures and strain rates is beyond the scope of this Letter, but see Ref. [17] for a possible direction to go. Also, in the follow up paper to this Letter we will present the theory for the asymmetry in the yield-strain as a function of ζ_n and ζ_k. Stay tuned.

Acknowledgements: this work was supported by the Israel Science Foundation, the German-Israeli Foundation and by the ERC under the STANPAS "ideas" grant.

[1] For extensive experimental evience see Y.F. Gao, L. Wang, H. Bei and T.G. Nieh, Acta Materiala, **59**, 4159 (2011), and references therein.
[2] J.W. Rudnicki and J. R. Rice, J. Mech. Phys. Solids, **23**, 371 (1975).
[3] M. Zhao and M. Li, Appl. Phys. Lett **93**, 241906 (2008).
[4] M. Zhao and M. Li, J. Mater. Res. **24**, 2688 (2008).
[5] C.E. Maloney and A. Lemaître, Phys. Rev. E **74**, 016118 (2006).
[6] A. Tanguy, F. Leonforte and J.L Barrat, Eur. Phys. J. **E20**, 355-364 (2006).
[7] R. Dasgupta, O. Gendelman, I. Procaccia and C. Shor "Shear localization in 3-Dimensional Amorphous Solids", to be submitted to PRE.
[8] E. Lerner and I Procaccia, Phys Rev E, **79**,066109 (2009).
[9] E. Lerner and I. Procaccia, Phys, Rev. E, **80**, 026128 (2009).
[10] S. Karmakar, A. Lemaître, E. Lerner and I. Procaccia, Phys. Rev. Lett. **104**, 215502 (2010).
[11] R. Dasgupta, H. G. E. Hentschel and I. Procaccia, Phys.Rev. Lett., **109** 255502 (2012).
[12] R. Dasgupta, H. G. E. Hentschel and I. Procaccia, Phys. Rev. E **87**, 022810 (2013).
[13] D. L. Malandro and D. J. Lacks, J. Chem. Phys. **110**, 4593 (1999).
[14] R. Dasgupta, S. Karmakar and I. Procaccia, Phys. Rev. Lett. **108**, 075701 (2012).
[15] J. D. Eshelby, Proc. R. Soc. Lond. A **241**, 376 (1957); **252**, 561 (1959).
[16] http://www.weizmann.ac.il/chemphys/cfprocac/publ.html

(papers online #191).

[17] R. Dasgupta, Ashwin J., H.G.E.Hentschel and I. Procaccia, Phys. Rev. B **87**, 020101(R) (2013).